Available online at www.sciencedirect.com

ScienceDirect

Procedia Engineering 102 (2015) 1539 – 1545

Procedia Engineering

www.elsevier.com/locate/procedia

The 7th World Congress on Particle Technology (WCPT7)

Numerical study of a bi-disperse gas-solid fluidized bed using an Eulerian and Lagrangian hybrid model

Simon Schneiderbauer[a]*, Stefan Puttinger[a], Stefan Pirker[a]

[a]*Department of Particulate Flow Modelling, Johannes Kepler University, Altenbergerstr. 69, A-4040 Linz, Austria*

Abstract

In this paper, we present a hybrid model for the numerical assessment of poly-disperse gas-solid fluidized beds. The main idea of such a modeling strategy is to use a combination of a Lagrangian discrete phase model (DPM) and a kinetic theory based TFM to take advantage of the benefits of those two different formulations. On the one hand, the local distribution of the different particle diameters, which is required for the gas-solid drag force, can be obtained by tracking statistically representative particle trajectories for each particle diameter class. On the other hand, the contribution from the inter-particle stresses, i.e. inter-particle collisions, can be deduced from the TFM solution. These then appear as additional body force in the force balance of the DPM. Note that in a first step we solely consider diameter averaged solids stresses since the drag force is at least on order of magnitude higher than the solids stresses in fluidized beds. Finally, the numerical model is applied to a fluidized bed of a bi-disperse mixture of glass particles (0.5 mm and 2.5 mm particles) and with a cross-section of 0.15 m x 0.02 m. The results are then analyzed with respect to experimental data of Puttinger et al [1]. This comparison demonstrates that the computed bed hydrodynamics is in fairly good agreement with the experiment. However, the results also suggest that sub-grid drag corrections [2–4] for poly-disperse fluidized beds are required to make the numerical investigation of industrial scale fluidized bed units accessible.

Selection and peer-review under responsibility of Chinese Society of Particuology, Institute of Process Engineering, Chinese Academy of Sciences (CAS)

Keywords: Two-fluid model (TFM); Fluidized bed; Particle segregation; Sub-grid drag modification; Discrete phase model (DPM);

* Corresponding author. Tel.: +43 732 24686482; fax: +43 732 24686462.
E-mail address: simon.schneiderbauer@jku.at

Selection and peer-review under responsibility of Chinese Society of Particuology, Institute of Process Engineering, Chinese Academy of Sciences (CAS)
doi:10.1016/j.proeng.2015.01.289

1. Introduction

Most industrial applications of fluidized bed reactors include poly-disperse materials [5,6]. Thus, it is important to understand the mixing and segregation of the particles in the reactor to evaluate its efficiency [1,7]. One of the most straight forward numerical methods to account for poly-disperse mixtures is DEM (discrete element method) [8]. However, since the total number of particles involved in most practically relevant fluidized beds is extremely large, it may be impractical to solve the equations of motion for each particle. It is, therefore, common to investigate particulate flows in large process units using averaged equations of motion, i.e. two-fluid models (TFM), which include the inter-particle collisions statistically by kinetic theory based closures of the particle stresses [9–11]. Even though each representative particle diameter requires an additional momentum and continuity equation, which considerably raises the computational demand with increasing number of particle diameters [5,12].

Furthermore, the TFM approach requires considerably fine grids since the minimum stable sizes of clusters and shear bands are around ten particle diameters [13]. Thus, due to computational limitations a fully resolved simulation of industrial scale reactors is still unfeasible. It is, therefore, common to use coarse grids to reduce the demand on computational resources. However, such a procedure inevitably neglects small (unresolved) scales, which leads, for example, to a considerable overestimation of the bed expansion in the case of fine particles. Many sub-grid drag modifications have, therefore, been put forth by academic researchers to account for the effect of small unresolved scales on the resolved meso-scales in this case [2,3,14–18].

In this paper, following [12,19] we therefore present a hybrid model for the numerical assessment of poly-disperse gas-solid fluidized beds. The main idea of such a modeling strategy is to use a combination of a Lagrangian discrete phase model (DPM) and a coarse-grained TFM to take advantage of the benefits of those two different formulations. Furthermore, sub-grid drag corrections [2–4] are applied to account for the impact of the small unresolved scales on the gas-solid drag force.

Nomenclature

$\beta_{\langle d\rangle}$	drag coefficient
β_{poly}	correction of drag force for poly-disperse mixtures
d_p	particle diameter (m)
$\langle d\rangle$	Sauter mean diameter (m)
e	coefficient of restitution (-)
ε_s	volume fraction of solid phase (-)
ρ_s	density of solid phase (kg/m^3)
$\mathbf{u}_{p,i}$	velocity of a Lagrangian tracer particle (m/s)
$\mathbf{u}_g$	local averaged velocity of solid phase (m/s)
$\mathbf{u}_s$	local averaged velocity of solid phase (m/s)
x_i	fraction of particle class i (-)

2. Modeling of poly-disperse gas-solid flows

2.1. Coarse grained kinetic theory based two-fluid model (cgTFM)

As in our earlier studies [4,6] we use a coarse-grained kinetic-theory based two-fluid model to study fluidization. This model has been proven to be applicable to industrial scale fluidized beds since it yields reasonable agreement of the bed expansion with experiments for bubbling and turbulent fluidized beds. Furthermore, even in the case of fast fluidization of Geldart A particles fairly good agreement with measurements of solids holdup and particle mass flux is achieved [4]. Recently, this coarse-grained kinetic-theory based two-fluid model has been extended to the

fluidization of poly-disperse mixtures [6]. However, these previous studies did not include the impact of segregation. Since these models are well documented in our previous studies [2–4,6], we do not repeat the details here.

2.2. Lagrangian disrete phase model (DPM)

The local distribution of the different particle diameters, which is required for the gas-solid drag force, can be obtained by tracking statistically representative particle trajectories for each particle diameter class along the solids flow obtained from the coarse-grained TFM. The momentum balance for such a "tracer" trajectory therefore reads

$$\frac{\mathbf{u}_{p,i}}{t} = -\frac{1}{\tau_{c,i}}(\mathbf{u}_{p,i} - \mathbf{u}_s) + \mathbf{F}_{poly,i} \,, \tag{1}$$

where $\mathbf{u}_{p,i}$ denotes the velocity of the Lagrangian tracer of particle diameter class i, $\mathbf{u}_s$ the solids velocity and $\tau_{c,i}$ is a collisional time scale required to accelerate a single particle to the average solids velocity $\mathbf{u}_s$ [12] (compare also with Figure 1)

$$\frac{1}{\tau_{c,i}} = \frac{3(1+e)}{4}\varepsilon_s \left\| \mathbf{u}_s - \mathbf{u}_{p,i} \right\| \sum_j^{N_{sp}} \frac{x_i \left(d_{p,i} + d_{p,j}\right)^2 g_{0,ij}}{d_{p,i}^3 + d_{p,j}^3}. \tag{2}$$

Here, e is the coefficient of restitution, ε_s the volume fraction of the solid phase, N_{sp} the number of diameter classes, $d_{p,i}$ the particle diameter of class i, $g_{0,ij}$ the radial distribution function including a multisize mixture of hard spheres at contact [5] and $x_i = \varepsilon_{s,i} / \varepsilon_s$, where $\varepsilon_{s,i}$ denotes the volume fraction of class i.

Since the tracers are allowed to have different physical properties (e.g. particle diameter) $\mathbf{F}_{poly,i}$ accounts for the difference of the drag force on a single particle to the drag force on the local ensemble of particles. In our previous study [12] we have shown that such an approach considerably reduces the computational cost compared to multi-fluid models, where each particle diameter class is represented by its own phase.

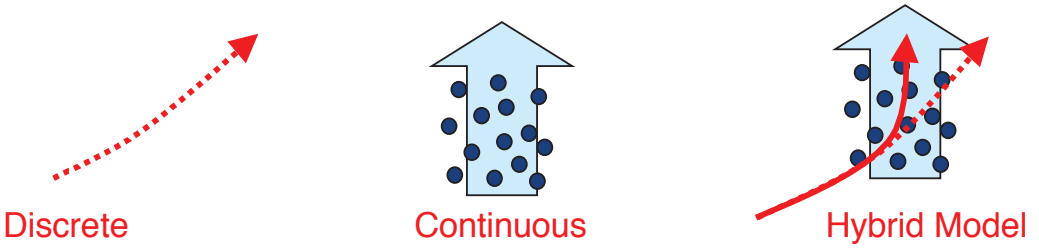

Fig. 1. From left to right: Trajectory of a single Lagrangian tracer particle; the continuous solid phase moves with locally averaged velocity; equation (3) accounts for the impact of the collisions of the Lagrangian trajectory with solid phase.

Following Beetstra et al. [20] the drag force per unit volume exerted on a poly-disperse mixture of spherical particle can be written as follows

$$\mathbf{F}_d = \beta_{\langle d \rangle} \beta_{poly} (\mathbf{u}_g - \mathbf{u}_s) \,, \tag{3}$$

where

$$\beta_{\langle d \rangle} = 18 \mu_g \varepsilon_s \varepsilon_g^2 F_{\langle d \rangle}(\varepsilon_g, \varepsilon_s, \mathrm{Re}_{\langle d \rangle}),$$

$$\beta_{poly} = \sum_{i=1}^{N_{sp}} \frac{x_i F_i}{d_{p,i}^2} \,.$$

Note the exact definitions of $F_{\langle d \rangle}$ and F_i can be found in [20,21]. Here, $\mathbf{u}_g$ denotes the gas-velocity, Re the particle Reynolds number. Above equation reveals that the drag force can be split into a part $\beta_{\langle d \rangle}$, which solely depends on the local solids volume fraction and the Sauter mean diameter $\langle d \rangle$ of the poly-disperse mixture and into a part β_{poly}, which accounts for effect of the different diameters with volume fraction $\varepsilon_{s,i}$. Thus, we find

$$\mathbf{F}_{poly,i} = \frac{1}{\varepsilon_s \rho_s} \beta_{\langle d \rangle} \left(\frac{F_i}{d_{s,i}^2} - \beta_{poly} \right) (\mathbf{u}_g - \mathbf{u}_s) , \tag{4}$$

Finally, the average diameter used in the TFM simulation is computed from

$$\langle d \rangle_{TFM} = \left(\sum_{i=1}^{N_{sp}} \frac{x_i}{d_{p,i}} \right)^{-1} ,$$

where the x_i's are determined from the distribution of the Lagragian tracer particles based on the Eulerian grid used for the TFM part. Note that in the case where no tracer particle is in a specific numerical cell we apply a diffusive smoothening approach to the exchange fields locally [22].

The contribution from the inter-particle stresses, i.e. inter-particle collisions, can be deduced from the coarse-grained TFM solution. These then determine the collisional time scale $\tau_{c,i}$ appearing in the momentum balances of the tracer particles. Note that in a first step we solely consider diameter averaged solids stresses since the drag force is at least on order of magnitude higher than the solids stresses in fluidized beds.

3. Numerical simulations

For the numerical simulation we use the commercial CFD-solver FLUENT (version 14), whereby we implemented the poly-disperse drag force [20] and the coarse grained solid stresses of [2–4,23] by using user defined functions. For the discretization of all convective terms a second-order upwind scheme is used. The derivatives appearing in the diffusion terms are computed by a least squares method and the pressure–velocity coupling is achieved by the SIMPLE algorithm. For further details the reader is referred to our previous work [2,3].

Finally, we use a grid resolution equal to three times the diameter of the largest particle fraction. However, such a coarse grid resolution inevitably neglects the small scale flow structures, i.e. sub-grid heterogeneities of the fine particles. Thus, we apply sub-grid modifications for the gas-solid drag force and the solids stresses to account for the effect of those small unresolved scales [2–4,23]. Note that one single tracer trajectory represents on the one hand a parcel of 64 0.5 mm particles and on the other hand, a parcel of 2 2.6 mm particles in the cases studied.

A correct numerical model should therefore be able to produce inhomogeneous bed segregation and a similar channel-building behavior when initialized by a local inhomogeneity in the particle mixture similar to the experiment.

4. Results

The numerical hybrid model is applied to a fluidized bed of a bi-disperse mixture of glass particles (0.5 mm and 2.5 mm particles) and with a cross-section of 0.15 m x 0.02 m. The initial mass fraction of the 0.5 mm particle was set homogenously to $x_i = 60\%$. To break symmetry we initialised a small area above the distributor blade with a partially smaller mass fraction of the 0.5 mm particles. Finally, the initial bed height was given by 0.2 m and the superficial gas velocities were 0.44 m/s and 0.76 m/s.

In Figure 2 a comparison of numerical and experimental results [1] for a superficial gas velocity of 0.44 m/s is shown. The results show that during settlement of the bed segregation occurs for this combination of particle sizes. Due to the initial inhomogeneity above the distributor plate, an area of large particles is formed right above this region.

The experimental data (Puttinger et al., 2014) further shows that this effect is reproducible for particle mixtures in the range $x_i = 40\%$ to $x_i = 60\%$ and superficial velocities in the range 0.4 to 0.5 m/s. The small particle fraction is

fluidized at this gas rate (minimum fluidization velocity 0.32 m/s) while the large particles are not (1.6 m/s). Therefore, the large particles do not move anymore as soon as they have settled in a certain place.

The comparison further demonstrates that the hybrid model yields (including bed expansion, segregation and channelling) fairly good agreement with experiments. Especially, the formation of the "dead man", which manifests a stationary accumulation of large particles in the centre, is predicted appropriately. The formation of this stationary zone leads to a partial de-fluidization. Only the small particles above the dead man remain fluidized.

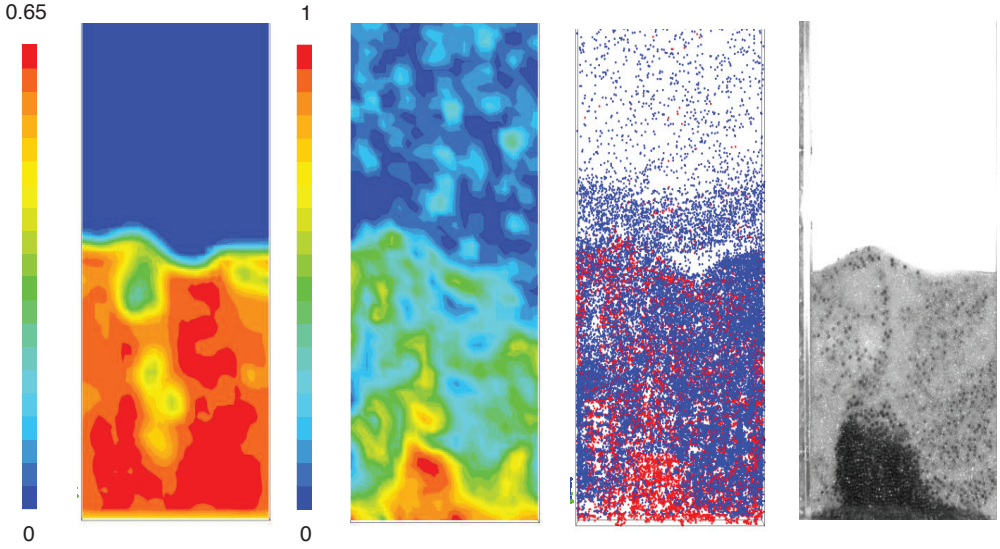

Fig. 2: Partial de-fluidization in a bi-disperse fluidized bed due to de-mixing of two particle classes for a superficial gas velocity of 0.44 m/s: Large (black) particles form a non-uniform packed bed just above the distributor plate; process gas channels to the upper part of the bubbling fluidized bed of small (gray) particles. From left to right: solid-phase volume fraction; fraction of large particles; tracer particles colored by their size (yellow: 0.5 mm; red: 2.6 mm); experimental observation.

Figure 3 shows the corresponding results for a superficial gas velocity of 0.76 m/s. In this case, the numerical hybrid simulation is able to reproduce the segregation pattern observed from the experiments as well (Figure 3d). Especially, the large particles tend to settle to the bottom of the bed, where they form a static bed (i.e. de-fluidization due to segregation) since their minimum fluidization velocity is much larger than the superficial gas velocity. Furthermore, the upper part of the bed remains fluidized, where it consists mostly of the 0.5 mm particles. In contrast to figure 2, no “dead man” forms in this case since the higher gas rate leads to a more pronounced bubbling behaviour impeding the formation of a static “dead man”. Finally, note that in this case the computed bed expansion cannot be compared to the experimental data since the simulation was initialized with a considerably higher static bed height than used in the experiments.

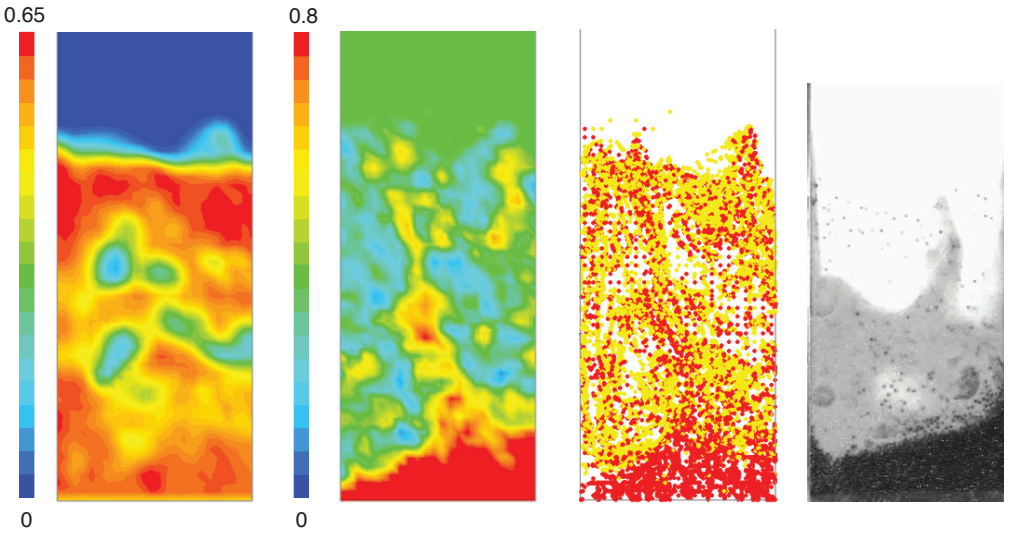

Fig. 3: Partial de-fluidization in a bi-disperse fluidized bed due to de-mixing of two particle classes for a superficial gas velocity of 0.76 m/s: Large (black) particles form a non-uniform packed bed just above the distributor plate; process gas channels to the upper part of the bubbling fluidized bed of small (gray) particles. From left to right: solid-phase volume fraction; fraction of large particles; tracer particles colored by their size (blue: 0.5 mm; red: 2.6 mm); experimental observation.

5. Conclusions

We have we presented a new hybrid Two Fluid Model (TFM) by additionally considering poly-disperse tracer particles. This includes the implementation of a poly-disperse drag law [20]. Furthermore, the spatial distribution of the Lagrangian tracer particles determines the average diameter required for TFM. Such a procedure allows to account for segregation in TFM efficiently. Finally, sub-grid modifications include the impact small unresolved scales when using coarse grids.

To conclude, the results clearly show that the hybrid TFM is able to picture segregation in poly-disperse gas-solid fluidized beds. Future efforts will concentrate on a quantitative comparison of the numerical simulations with experiments.

Acknowledgements

This work was funded by the Christian-Doppler Research Association, the Austrian Federal Ministry of Economy, Family and Youth, and the Austrian National Foundation for Research, Technology and Development.

References

[1] S. Puttinger, S. Schneiderbauer, L. von Berg, S. Pirker, in:, Proc. 7th World Congr. Part. Technol., Beijing, China, 2014, p. 6.
[2] S. Schneiderbauer, S. Puttinger, S. Pirker, AIChE J. 59 (2013) 4077.
[3] S. Schneiderbauer, S. Pirker, AIChE J. 60 (2014) 839.
[4] S. Schneiderbauer, S. Pirker, J. Comput. Multiph. Flows 6 (2014) 29.
[5] H. Iddir, H. Arastoopour, AIChE J. 51 (2005) 1620.
[6] S. Schneiderbauer, S. Puttinger, S. Pirker, P. Aguayo, V. Kanellopoulos, Submitt. to I&EC Res. (2013) 1.
[7] S. Puttinger, S. Schneiderbauer, L. von Berg, S. Pirker, in:, Proc. 11th Int. Conf. Fluid. Bed Technol., Beijing, China, 2014, p. 6.
[8] C. Goniva, C. Kloss, N.G. Deen, J.A.M. Kuipers, S. Pirker, Particuology 10 (2012) 582.
[9] C.K.K. Lun, S.B. Savage, D.J. Jeffrey, N. Chepurniy, J. Fluid Mech. 140 (1984) 223.
[10] K. Agrawal, P.N. Loezos, M. Syamlal, S. Sundaresan, J. Fluid Mech. 445 (2001) 151.
[11] S. Schneiderbauer, A. Aigner, S. Pirker, Chem. Eng. Sci. 80 (2012) 279.
[12] D. Schellander, S. Schneiderbauer, S. Pirker, Chem. Eng. Sci. 95 (2013) 107.

[13] A.T. Andrews, P.N. Loezos, S. Sundaresan, Ind. Eng. Chem. Res. 44 (2005) 6022.
[14] Y. Igci, S. Sundaresan, Ind. Eng. Chem. Res. 50 (2011) 13190.
[15] J.-F. Parmentier, O. Simonin, O. Delsart, AIChE J. 58 (2012) 1084.
[16] K. Hong, W. Wang, Q. Zhou, J. Wang, J. Li, Chem. Eng. Sci. 75 (2012) 376.
[17] C.C. Milioli, F.E. Milioli, W. Holloway, K. Agrawal, S. Sundaresan, AIChE J. 59 (2013) 3265.
[18] J. Wang, M.A. van der Hoef, J.A.M. Kuipers, Chem. Eng. Sci. 65 (2010) 2125.
[19] S. Pirker, D. Kahrimanovic, C. Kloss, B. Popoff, M. Braun, Pow. Techn. 204 (2010) 203.
[20] R. Beetstra, M.A. Van der Hoef, J.A.M. Kuipers, AIChE J. 53 (2007) 489.
[21] M.A. van der Hoef, M. van Sint Annaland, N.G. Deen, J.A.M. Kuipers, Annu. Rev. Fluid Mech. 40 (2008) 47.
[22] S. Pirker, D. Kahrimanovic, C. Goniva, Appl. Math. Model. 35 (2011) 2479.
[23] S. Schneiderbauer, S. Puttinger, S. Pirker, P. Aguayo, V. Kanellopoulos, Submitt. to I&EC Res. (2014).